Journal of Molecular Catalysis B: Enzymatic 61 (2009) 303–308

Contents lists available at ScienceDirect

Journal of Molecular Catalysis B: Enzymatic

journal homepage: www.elsevier.com/locate/molcatb

# Peroxidase-like activity of *Thermobifida fusca* hemoglobin: The oxidation of dibenzylbutanolide

Roberta Torge[a], Alessandra Comandini[b], Bruno Catacchio[b], Alessandra Bonamore[b], Bruno Botta[a], Alberto Boffi[b,*]

[a] *Istituto Pasteur Fondazione Cenci Bolognetti, Department of Chemistry and Technology of Drugs, University "Sapienza", P.le Aldo Moro 5, 00185 Rome, Italy*
[b] *Istituto Pasteur Fondazione Cenci Bolognetti, Department of Biochemical Sciences, University "Sapienza", P.le Aldo Moro 5, 00185 Rome, Italy*

ARTICLE INFO

*Article history:*
Received 31 March 2009
Received in revised form 7 August 2009
Accepted 18 August 2009
Available online 26 August 2009

*Keywords:*
*Thermobifida fusca*
Truncated hemoglobin
Dehydrogenation
Dibenzylbutanolides
Etoposide

ABSTRACT

The thermostable truncated hemoglobin from the actinomyces *Thermobifida fusca* (Tf-trHb) displays a robust peroxidase activity, with optimum at acidic pH values, in experiments with the redox mediator ABTS. However, typical peroxidase substrates, such as phenolic or aromatic amine compounds, appear to be poor substrates for Tf-trHb. In turn, the protein is able to catalyze a unique dehydrogenation reaction of dibenzylbutanolides, suggested intermediates in the biosynthesis of podophyllotoxin, in the presence of hydrogen peroxide. Dibenzylbutanolides with a free 4″-hydroxyl group were thus converted into the corresponding 2,7″-dehydroderivatives thus setting up the basis for an efficient biotransformation of this important precursor. In particular, Tf-trHb mediated oxidation of *trans*-2-(4″-hydroxy-3″,5″-dimethoxybenzyl)-3-(3′,4′-methylenedioxy-7′β-hydroxybenzyl)butanolide **1** into the corresponding benzylidene-benzoyl-γ-butyrolactone **2** was obtained at high yield and with excellent selectivity.

© 2009 Elsevier B.V. All rights reserved.

## 1. Introduction

Truncated hemoglobins are ubiquitous heme-containing proteins isolated from bacteria, fungi and yeasts [1]. The three-dimensional structure of these proteins is characterized by a two-over-two alpha helical sandwich instead of the typical three-over-three motif of vertebrate globins. However, in spite of the absence of the A and H helices, the topological positions that govern the heme–globin interaction are similar to those of classical globins and the overall nomenclature of key residues along the helices is readily superimposable. Thus, a proximal histidine residue in position F8 represent the only covalent link between heme and globin. The distal heme pocket is build up around three residues that are in close contact with the iron bound ligand, namely a tryptophan and a tyrosine lying parallel to the heme plane (WG8 and YCD1) and a second tyrosine (YB10), perpendicular to the heme plane, whose phenol hydroxyl points towards the iron bound ligand (see Fig. 1). The biological roles of truncated hemoglobins in bacteria are still uncertain though several lines of evidence indicate that these proteins are structurally and functionally related to heme peroxidases [2,3]. *Mycobacterium tuberculosis* truncated hemoglobin (trHbO) has been recently shown to possess a genuine peroxidase activity [3] in steady-state kinetic experiments in the presence of $H_2O_2$ and the one-electron acceptor ABTS. Moreover, trHbO has been shown to react with $H_2O_2$ to give a transient Compound I intermediate that is rapidly converted to a species with heme in the ferric state and two protein radicals through oxidation of aromatic side chains within the distal heme pocket (YCD1 and WG8). Optical stopped-flow experiments revealed a transient oxoferryl intermediate, whereas EPR spectroscopy provided evidence for both tyrosyl and tryptophanyl radicals [3]. These observations suggested that trHbO is designed to perform redox reactions due to the presence of the electron-rich oxidizable residues YCD1, and WG8 in the distal heme pocket. However, no clues are presently available that pave the way to the identification of possible physiological substrates for trHbO.

*Thermobifida fusca* truncated hemoglobin (Tf-trHb) can be considered as a thermostable analogue of trHbO in that it shares all relevant residues within the heme pocket in common with the latter protein (see Fig. 1) [4]. Accordingly, in preliminary experiments, Tf-trHb has been shown to possess a peroxidase-like activity that parallels that observed in trHbO. The observed activity prompted the present investigation aimed both at understanding the biochemical significance of the peroxide based catalysis and at exploiting the enzymatic capabilities of the protein in oxidative biotransformations. In this framework, a collection of substrates has been screened for peroxidase-like activity in the presence of Tf-trHb and hydrogen peroxide. Unexpectedly, compounds of the

* Corresponding author. Tel.: +39 06 4991 0990; fax: +39 06 4440 062.
*E-mail address:* alberto.boffi@uniroma1.it (A. Boffi).

1381-1177/$ – see front matter © 2009 Elsevier B.V. All rights reserved.
doi:10.1016/j.molcatb.2009.08.010

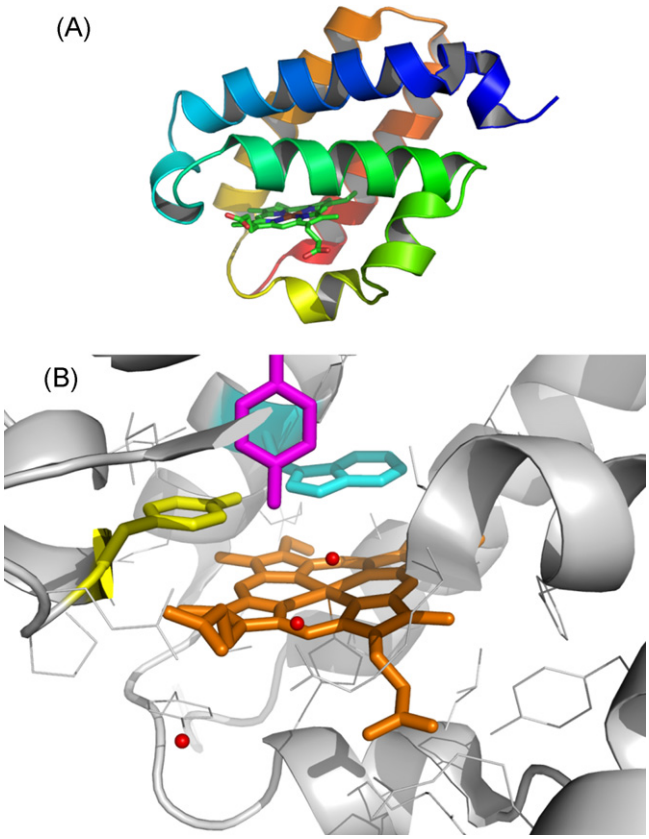


**Fig. 1.** Active site structure of *Thermobifida fusca* truncated hemoglobin. The overall structure of Tf-trHb is shown in panel A, a close-up view of the active site is depicted in panel B where the relevant aminoacids of the distal heme pocket are represented in sticks: WG8 cyan, YB10 magenta and YCD1 yellow. PDB coordinates: 2BMM, pictures were done using Pymol software (DeLano scientific). (For interpretation of the references to color in this figure legend, the reader is referred to the web version of the article.)

dibenzylbutanolide family were found to be the best substrates for Tf-trHb. This result is of high interest in that dibenzylbutanolides are important intermediates for the synthesis of high valued anti-cancer drugs such as etoposide, etophos and teniposide.

## 2. Experimental

### 2.1. Materials

Horseradish peroxidase (HRP), ABTS and $H_2O_2$ (30%, v/v) were obtained from Sigma. The concentration of $H_2O_2$ stock solution was determined spectrophotometrically at 240 nm ($\varepsilon = 43.5\ M^{-1}\ cm^{-1}$). HDMB-butanolide (*trans*-2-(4″-hydroxy-3″,5″-dimethoxybenzyl)-3-(3′,4′-methylenedioxy-7′β-hydroxybenzyl)butanolide) **1** was prepared according to Ref. [6] $^1H$ and $^{13}C$ NMR spectra were collected on a Bruker Avance spectrometer (400 MHz).

### 2.2. Optical absorption spectroscopy

Optical absorption spectra and single wavelength kinetic experiments were carried out using a Jasco V-560 spectrophotometer (Jasco Inc., Japan) equipped with a temperature controlled cell holder. The UV molar absorptivity of the HDMB oxidized product was estimated 680 $M^{-1}\ cm^{-1}$ at 336 nm. The molar absorptivity of Tf-trHb was 144.000 $M^{-1}\ cm^{-1}$ at 408 nm for the ferric derivative at pH 7.0 [4].

### 2.3. T. fusca truncated hemoglobin and its mutants

The truncated hemoglobin from *T. fusca* was overexpressed in standard BL-21 DE3 cells and purified as described previously [4]. A set of mutants were obtained by site directed mutagenesis using standard procedures by using the QuickChange site directed mutagenesis kit (Stratagene, La Jolla, CA, USA) [5]. In particular, each of the three residues within the distal heme pocket (WG8, YCD1 and YB10) was mutated to a phenylalanine thus yielding the following: WG8F, YCD1F, YB10F, the double mutant YB10F-WG8F and the triple mutant WG8F-YCD1F-YB10F. Each mutant was then expressed and purified under the same experimental conditions of the native protein.

### 2.4. Peroxidase activity measurements with ABTS

Steady-state kinetic constants for the oxidation of ABTS were obtained by measuring the initial rates as a function of $H_2O_2$ concentration at pH values of 5.5, 6.1, 6.5, 7.0, 7.5 and 8.0. ABTS and buffer were equilibrated within the thermostatted cuvette (3 ml) in the spectrophotometer under stirring, thereafter, 5 μl of Tf-trHb stock solution were added, measurements were started after 10 s and followed over 5 min. The signal increase was linear up to 4–5 min. The formation rate of the ABTS oxidation product was determined from the increase in the absorbance at 405 nm using a molar extinction coefficient of $3.6 \times 10^4\ M^{-1}\ cm^{-1}$ [2]. Data fitting was performed according to standard least squares methods using the Matlab program (The Mathworks Inc., South Natick, MA).

### 2.5. HDMB-butanolide oxidation

Experiments were performed in 0.1 M sodium phosphate buffer at pH 7.0 and 25 °C. HDMB-butanolide (*trans*-2-(4″-hydroxy-3″,5″-dimethoxybenzyl)-3-(3′,4′-methylenedioxy-7′β-hydroxybenzyl) butanolide) **1** was first dissolved in 2-methoxyethanol and then added to a solution containing the aqueous buffer and hydrogen peroxide. Typically, 6–60 μl of HDMB-butanolide **1** in 2-methoxyethanol were added to 850 μl of 0.1 M sodium phosphate buffer at pH 7.0 (2 mg/ml, 0.3 mM final) and 70 μl of 0.1 M hydrogen peroxide, (final concentration 0.7–7 mM). Tf-trHb was then added to the solution to a final concentration of 1 μM. The reaction mixture was placed in a 0.5 cm quartz cell and the time course of the reaction was followed at 336 nm over 30 min.

The preparative reaction was carried out on a solution of *trans*-2-(4″-hydroxy-3″,5″-dimethoxybenzyl)-3-(3′,4′-methylenedioxy-7′β-hydroxybenzyl)butanolide **1** (12.5 ml, 4 mg/ml in 2-methoxyethanol) (0.3 mM final), 8 ml of recombinant enzyme Tf-trHb 100 μM (2.3 μM final concentration). 4.7 ml of hydrogen peroxide 0.04 M (0.5 mM final) were sequentially added to 325 ml of 0.1 M sodium phosphate buffer at pH 7.0. The reaction mixture was stirred for 4 h at 25 °C. The resulting solution was extracted with chloroform, the combined organic layers were dried on sodium sulphate and concentrated in vacuo. The crude product was purified by silica gel column chromatography packed initially with hexane/ethylacetate 5:5 and forerunning with hexane/ethylacetate 2:3, yielding the pure dehydrogenation product **2** (60%).

**Compound 2**. $^1H$ NMR (400 MHz, $CDCl_3$, 25 °C) $\delta$: 7.60 (1H, br s; H-7″), 7.06 (2H, s; H-2″, H-6″), 6.81, 6.75 (1H + 2H, m + m, $AB_2$ system; H-2′, H-5′, H-6′), 5.97, 5.95 (1H + 1H, d + d, $J = 1$ Hz; $OCH_2O$), 4.98 (1H, d, $J = 6$ Hz, H-7′), 4.41 (1H, br d, $J = 9$ Hz, H-4a), 4.22 (1H, dd, $J = 9$ and 7 Hz; H-4b), 3.99 (1H, br t, $J = 6.5$ Hz; H-3), 3.98 (6H, s; 2× OMe). $^{13}C$ NMR (400 MHz, $CDCl_3$, 25 °C) $\delta$: 172.36, 148.04, 147.84, 147.13, 139.51, 137.10, 133.79, 125.28, 122.82, 120.04, 108.28, 107.38, 106.56, 101.28, 73.91, 66.85, 56.41, 45.48.

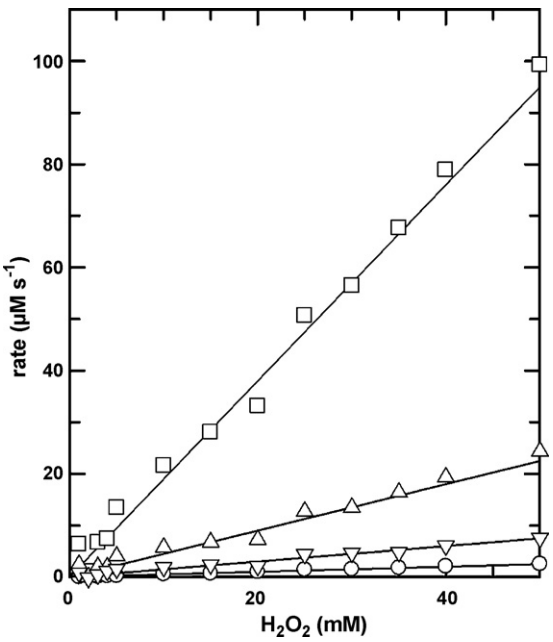


**Fig. 2.** Steady-state kinetics of the oxidation reaction of ABTS with Tf-trHb. ABTS (1 mM) oxidation by native trTfHb (squares) and its WG8F (triangles), YCD1F (reverted triangles) and WG8F-YCD1F-YB10F (open circles) mutants in the presence of $H_2O_2$. The initial rates estimated from the time courses of the reaction were measured at 405 nm as a function of $H_2O_2$ concentrations at pH 7.0 and 25 °C. Protein concentration was 0.1 μM.

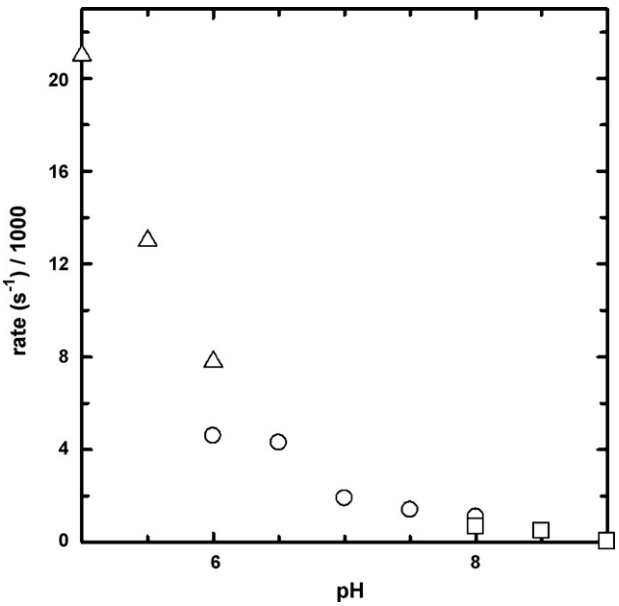


**Fig. 3.** pH dependence of the peroxidase activity in *Thermobifida fusca* truncated hemoglobin. Steady-state kinetic constants for the oxidation of ABTS were obtained by measuring the initial rates as a function of $H_2O_2$ concentration at 25 °C at pH values of 5.5, 6.1, 6.5, 7.0, 7.5 and 8.0 in 0.1 M citrate buffer (triangles), 0.1 M phosphate buffer (circles) or 0.1 M Tris–HCl buffer (squares). Each experimental point represent the slope of the line obtained as described in Fig. 2.

ESI-MS (negative) *m/z*: 399.1 $[M-H]^-$, 385.2 $[M-CH_3]^-$, 355 $[M-CO_2]^-$, 339 $[M-2OCH_3]^-$, 293, 249, 236, 205 $[249-CO_2]^-$, 190 $[205-15]^-$, 175 $[190-15]^-$, 161.

UV nm: 289, 336; $\varepsilon_{336}$: 680 $M^{-1}$.

## 3. Results

### 3.1. Steady-state kinetics of ABTS oxidation

Tf-trHb peroxidase activity was measured by following the time course of the one-electron oxidation of ABTS to its corresponding radical cation. Time courses were followed at 405 nm using varying amounts of $H_2O_2$. The apparent rate of the reaction of was obtained from the slope of the plot of initial velocity as a function of $H_2O_2$ concentration (Fig. 2). The apparent first-order dependence on $H_2O_2$ concentration was $1900 \pm 21\ M^{-1}\ s^{-1}$, similar to that observed for trHbO (see Table 1). The overall activity is decreased in the single mutants WG8F and YCD1F and nearly abolished in the triple mutant (WG8F-YCD1F-YB10F). It should be mentioned that other mutants involving substitution of YB10 (YB10F and YB10F-WG8F) led to non-functional proteins with spectral characteristics typical of sulfoheme derivatives (data not shown).

**Table 1**
Apparent first-order dependence on $H_2O_2$ concentration with ABTS substrate for Tf-trHb and its mutants.

| Protein | $k_{app}$ ($M^{-1}\ s^{-1}$) |
|---|---|
| Tf-trHb wild type | $1900 \pm 21$ |
| WG8F | $767 \pm 31$ |
| YCD1F | $814 \pm 39$ |
| YB10F | $160 \pm 33$ |
| WG8F-YCD1F-YB10F | n.d. |
| YB10F-WG8F | 10< |
| Mt-trHb | $1500 \pm 20$[a] |

Experimental conditions: protein concentration, 3 μM, hydrogen peroxide 0.5 mM, in 0.1 M sodium phosphate buffer at pH 7.0, temperature 25 °C.

[a] Data from Ouellet et al.

### 3.2. Substrate screenings for peroxidase activity

A collection of 32 substrates was analyzed for the peroxidase activity of Tf-trHb by TLC screenings in parallel with HRP as a control. In a few cases, Tf-trHb mediated oxidation gave rise to different products with respect to HRP, as judged from the relative positions of the products on the TLC plates. Oxidation of substrates of the anthraquinone family (alyzarine, emodyne, and ferruginin) and substituted benzylbutanolides or chalcones yielded relatively homogeneous products, distinct from those observed in analogous reactions with HRP. Compounds of the benzylbutanolide family, in particular, afforded single reaction products in good yields (>50%). In turn, results obtained with typical phenolic substrates (cathecoles, naphtoquinones, chalcones and flavonoids) or aromatic amines (substituted anilines) were essentially superimposable to those obtained with HRP (see supplementary information) although products were obtained at significantly lower yields.

Thus, HDMB-butanolide **1** was chosen as a substrate for further investigation in order to characterize the reaction product and evaluate the oxidation kinetics. In UV–vis spectral characterization, the absorption profiles of HDMB-butanolide **1** were analyzed after addition of Tf-trHb and hydrogen peroxide at pH 7.0 and 25 °C (see Fig. 4A). Absorption peaks of at 284 nm were found for HDMB-butanolide **1** whereas a maximum at 334 nm with a shoulder at 284 nm was present in the UV–vis spectrum of the oxidation product. The time courses of the reaction were also analyzed at fixed wavelength (336 nm) as a function of hydrogen peroxide concentration (Fig. 4B). The observed time courses displayed a second order behavior as a function of hydrogen peroxide but, at variance with those of ABTS oxidation, were non-linear. Addition of fresh enzyme did not improve the overall reaction yield thus suggesting a product inhibition phenomenon. Nevertheless, optimal reaction

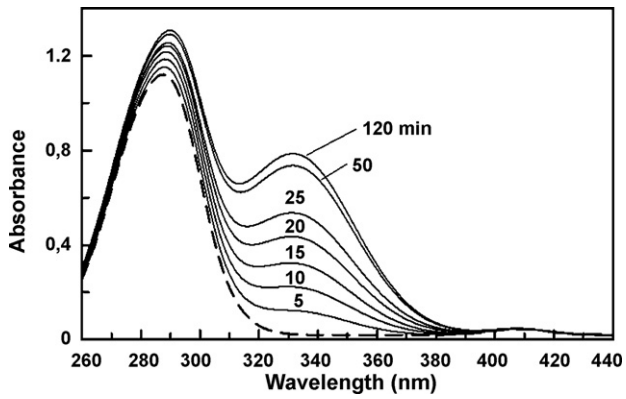


**Fig. 4.** Kinetics of the oxidation reaction of HDMB-butanolide with Tf-trHb. Spectra are reported at constant time intervals after Tf-trHb addition to the substrate solution containing hydrogen peroxide. Experimental conditions were: HDMB-butanolide (0.1 mM); Tf-trHb (1 μM) in the presence of $H_2O_2$. Experiments were run at 25 °C in 0.1 M phosphate buffer at pH 7.0.

conditions were found at pH 7.0 and 25 °C where kinetics is slower than at acidic pH values but the overall yield is better.

Thus, *trans*-2-(4″-hydroxy-3″,5″-dimethoxybenzyl)-3-(3′,4′-methylenedioxy-7′β-hydroxybenzyl)butanolide **1**[15] was treated with Tf-trHb in the presence of $H_2O_2$ in a preparative reaction vessel under the conditions reported in Section 2. The product was identified by $H^1$NMR, EIMS, infrared and UV spectroscopy as benzylidene-benzoyl-γ-butyrolactone **2** (Fig. 5) with 60% yields. NMR spectra of **2** indicated the formation of a double bond between C2–C7″ carbons (see Table 2), and the values of the isolated olefinic protons H-7″, H-3′, and H2–H4 are consistent with an *E* configuration.

The structure of **2** was then confirmed by the molecular peak in the ESI-MS spectrum at *m*/*z* 399 ([M−H]$^-$), two units lower than precursor **1** (Table 3). Notably, the same type of reaction did not occur with the commercial horseradish or soybean peroxidase HRP in the presence of $H_2O_2$.

**Table 2**
$^{13}$C and $^1$H NMR spectral data of compounds **1**, **2**[a].

| | **1** | | **2** | |
|---|---|---|---|---|
| | $\delta_C$ | $\delta_H$ | $\delta_C$ | $\delta_H$ |
| 7′ | 75.15 | 4.62 d | 73.91 | 4.98 d |
| 1 | 170.04 | | 172.36 | |
| 4′ | 148.03 | | 148.04 | |
| 3′ | 147.47 | | 147.84 | |
| 3″,5″ | 146.80 | | 147.13 | |
| 1″ | 128.41 | | 125.28 | |
| 1′ | 135.40 | | 133.79 | |
| 4″ | 133.29 | | 137.10 | |
| 6′ | 119.18 | 6.69 d br | 120.04 | 6.75 m |
| 2′ | 106.06 | 6.66 s br | 108.28 | 6.81 m |
| 5′ | 108.12 | 6.74 d | 106.56 | 6.75 m |
| 2″,6″ | 106.24 | 6.37 s | 107.38 | 7.06 s |
| $OCH_2O$ | 101.29 | 5.97 d | 101.28 | 5.97 d |
| | | 5.90 d | | 5.95 d |
| 4 | 68.39 | 3.95 dd | 66.85 | 4.41 d br |
| | | 3.93 dd | | 4.22 dd |
| OMe | 56.20 | 3.84 s | 56.41 | 3.98 s |
| 3 | 44.80 | 3.02–2.60 m | 45.48 | 3.99 t br |
| 2 | 43.72 | 3.02–2.60 m | 122.82 | |
| 7″ | 35.37 | 3.02–2.60 m | 139.51 | 7.60 br s |

[a] 400 MHz ($^1$H) and 400 MHz ($^{13}$C); $CDCl_3$, TMS as int. stand.; room temp. In the proton spectra all the signals showed the appropriate integrated intensity.

**Table 3**
MS spectral data[a] of substrate (**1**) and biotransformation product (**2**).

| Compound **1** | Compound **2** |
|---|---|
| 402 $[M]^+$ | 399.1 $[M-H]^-$ |
| 401 $[M-H]^+$ | 385.2 $[M-CH_3]^-$ |
| 384 $[M-H_2O]^+$ | 355 $[M-CO_2]^-$ |
| 229 | 339 $[M-2OCH_3]^-$ |
| 178 | 293 |
| 167 $[B\text{-}Trop]^+$ | 249 |
| 151 $[A\text{-}CHOH]^+$ | 236 |
| 135 $[A\text{-}Trop]^+$ | 205 $[249-CO_2]^-$ |
| 122 | 190 $[205-15]^-$ |
| | 175 $[190-15]^-$ |
| | 161 |

[a] For **1**, ESI-MS (positive); for **2**, ESI-MS (negative).

## 4. Discussion

The data obtained in the present investigation highlight two distinct results that are of interest in the field of peroxidase chemistry and in oxidative biotransformation. The first result is an extension of previous findings on the truncated hemoglobin from *M. tuberculosis* [3]. The robust peroxidase activity of Tf-trHb, as determined in the ABTS oxidation experiments of Fig. 2, parallels that observed for trHbO thus suggesting that the unusual radical generation and electron delivery systems is conserved in the two truncated hemoglobins (Fig. 3). The twentyfold increase in the rate of ABTS oxidation from pH 7.0 to pH 5.0 of Tf-trHb peroxidase indicates that a protonation within the active site must have a role in $H_2O_2$ processing thus suggesting that the two phenolic groups of tyrosines YCD1 and YB10 may mimick the histidine-arginine couple operative in classical plant peroxidases. This is further supported

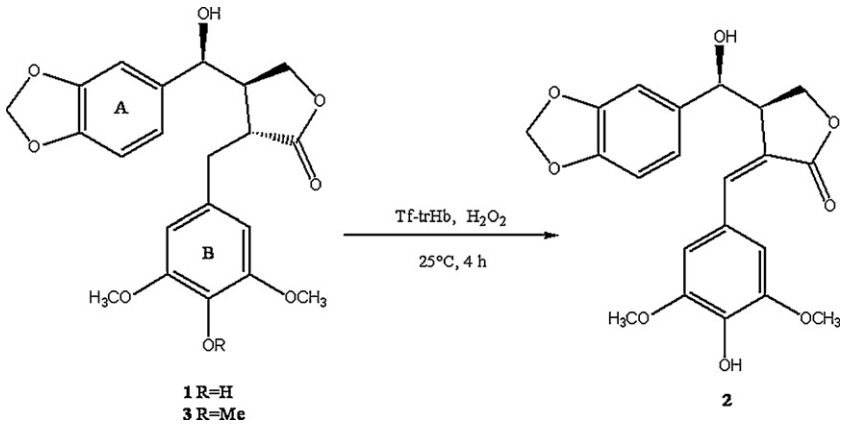


**Fig. 5.** Structures of HDMB-butanolide **1** and its oxidation product **2**. Structure of *trans*-2-(4″-hydroxy-3″,5″-dimethoxybenzyl)-3-(3′,4′-methylenedioxy-7′β-hydroxybenzyl)butanolide and formation of the corresponding benzylidene-benzoyl-γ-butyrolactone **2** are shown.

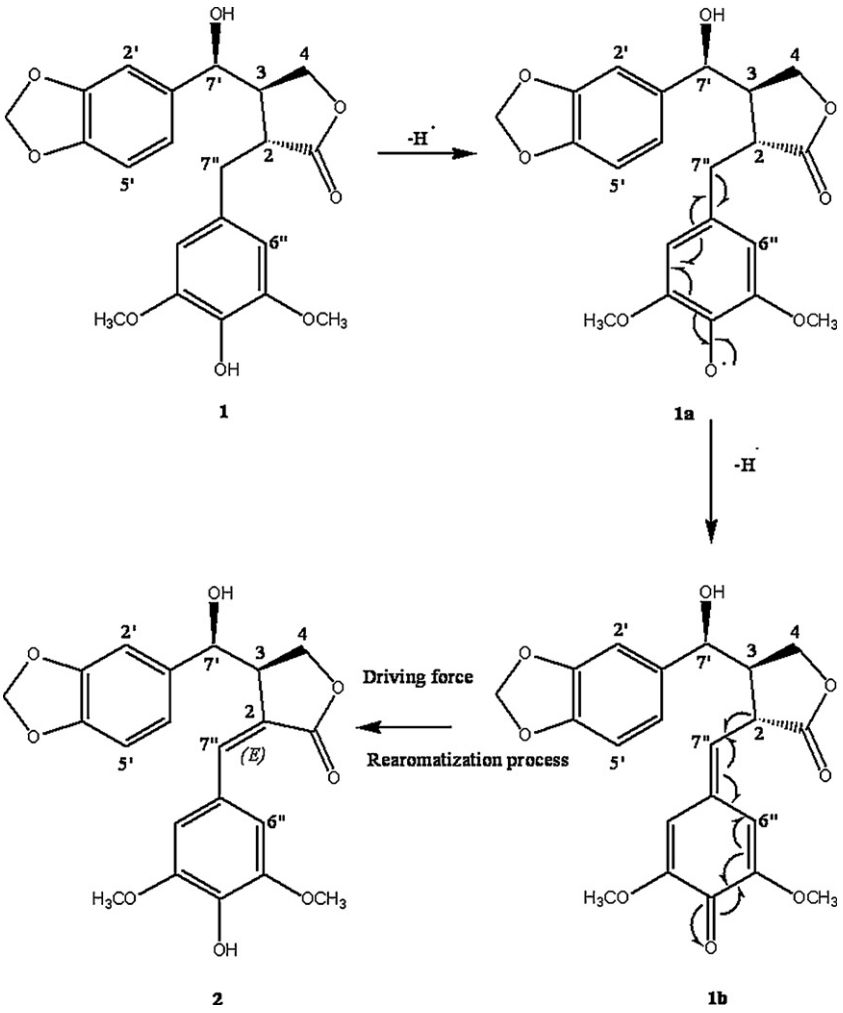


**Fig. 6.** Scheme of the oxidation/dehydrogenation of HDMB-butanolide substrate and suggested mechanism. The first two steps are in common with the proposed mechanism for the cyclization described in Ref. [6].

by the significant decrease of peroxidase activity in single YCD1F or YB10F mutants (see Table 1). Further mechanistic studies will be necessary to clarify the specific role of the two phenol rings and the proposed contribution of tryptophan WG8 as an "electron reservoir" within the catalytic process. As a general comment, within the small range of substrates screening carried out in the present work, it appears that Tf-trHb is a less efficient peroxidase with respect to the highly active horseradish peroxidase when exposed to typical phenolic substrates (lignin precursors). This is not unexpected in view of the lack of a metabolic pathway assimilable to that of lignin in bacteria and leaves the physiological function of bacterial hemoglobins an open question.

The second result concerns the efficiency of the Tf-trHb mediated oxidation of HDMB-butanolide **1**. The oxidative coupling of dibenzylbutanolides to the aryltetralin system of podophyllotoxin, had been addressed previously by means of specific plant peroxidases. Peroxidase enzymes produced within plant cell cultures [6–9] have also been employed by Kutney and coworkers for the synthesis of podophyllotoxin intermediates [10]. In fact, plant peroxidases usually catalyze radical reactions leading to C–C coupling between electron-rich centers which can form resonance stabilized radicals by loss of hydrogen atoms. The C-1β, C-2β, C-3α configuration of podophyllotoxin (**2**, Fig. 2) is of crucial importance for biological activity, whereas the stereochemistry at C-4 is of less concern due to the ease of isomerization [11]. A peroxidase enzyme from *Cassia didymobotrya* was able to catalyze the oxidation of 4,3′,4′-trihydroxychalcone and 4, 3′,4′-trihydroxy-3-methoxychalcone to the corresponding 3,3′-biflavanones, as mixtures of racemic and meso forms. In contrast, Tf-trHb has been shown to be able to perform a milder but more controlled oxidation reaction on dibenzylbutanolide systems.

The obtainment of **2** can be explained according to the dehydrogenation mechanism shown in Fig. 6. Presumably, the C2-C7″(*E*)-double bond formation is initiated by hydrogen atom abstraction from dibenzylbutanolide **1** to form the phenoxy radical **1a**, and the latter proceeds to a further abstraction from the benzylic carbon C-7″ leading to *p*-quinoid intermediate **1b**, which is expected to rapidly rearrange to the more stable aromatic compound **2**. The driving force of step **1b** → **2** is a rearomatization process through the abstraction and subsequent capture of the hydrogen H-2, in α position to the carbonyl group.

In order to support the mechanism hypothesized in Fig. 6, trimethoxybenzyl derivative **3** (Fig. 5) was incubated with Tf-trHb, but no biotransformation product was obtained. This finding supports the requirement of a free hydroxyl group in ring B to allow radical formation, and in turn formation of the *p*-quinoid intermediate **1b**.

## 5. Conclusions

The present data highlight the possible biocatalytic applications of novel peroxidase-like proteins, namely the truncated

hemoglobins of bacterial origin. Interestingly, these proteins are able to perform milder but more controlled oxidation reactions on selected substrates, different from those typical of horseradish or soybean peroxidases. Thus, the observed selective dehydrogenation reaction catalyzed by *T. fusca* truncated hemoglobin on the dibenzylbutanolide substrate paves the way to novel enzyme catalyzed radicalic reactions on complex phenolic systems.

## Acknowledgments

Project FIRB 2003 from MUR to A.B. and B.B. is gratefully acknowledged. FIRST grant n. RBIP067F9E and FIRB grant n. RBPR05NWWC_006 are acknowledged by B.B.

## Appendix A. Supplementary data

Supplementary data associated with this article can be found, in the online version, at doi:10.1016/j.molcatb.2009.08.010.

## References

[1] J.B. Wittenberg, M. Bolognesi, B.A. Wittenberg, M. Guertin, J. Biol. Chem. 277 (2002) 871–874.
[2] M. Kvist, E.S. Ryabova, E. Nordlander, L. Bülow, J. Biol. Inorg. Chem. 12 (2007) 324–334.
[3] H. Ouellet, K. Ranguelova, M. Labarre, J.B. Wittenberg, B.A. Wittenberg, R.S. Magliozzo, M. Guertin, J. Biol. Chem. 282 (2007) 7491–7503.
[4] A. Bonamore, A. Ilari, L. Giangiacomo, A. Bellelli, V. Morea, A. Boffi, FEBS J. 272 (2005) 4189–4201.
[5] M. Nelson, M. McClelland, Methods Enzymol. 216 (1992) 279–303.
[6] J.P. Kutney, Y.P. Chen, S. Gao, G.M. Hewitt, N.M. Stoynov, Heterocycles 36 (1993) 13.
[7] B. Botta, V. Vinciguerra, M.C. De Rosa, R. Scurria, A. Carbonetti, F. Ferrari, G. Delle Monache, D. Misiti, Heterocycles 29 (1989) 2175–2183.
[8] A. Vitali, B. Botta, G. Delle Monache, S. Zappitelli, P. Ricciardi, S. Melino, R. Petruzzelli, B. Giardina, Biochem. J. 331 (1999) 513–519.
[9] B. Botta, G. Delle Monache, P. Ricciardi, A. Vitali, V. Vinciguerra, D. Misiti, J.P. Kutney, N. Stoynov, Heterocycles 43 (1996) 2443–2456.
[10] J.P. Kutney, X. Du, R. Naidu, N. Stoynov, M. Takemoto, Heterocycles 42 (1996) 479–484.
[11] B. Botta, G. Delle Monache, D. Misiti, A. Vitali, G. Zappia, Curr. Med. Chem. 8 (2001) 1363–1381.